# Bulk Undoped GaAs–AlGaAs Substrate-Removed Electrooptic Modulators With 3.7-V-cm Drive Voltage at 1.55 $\mu$m

JaeHyuk Shin, Shaomin Wu, and Nadir Dagli, *Fellow, IEEE*

***Abstract*—Substrate removed bulk GaAs–AlGaAs electrooptic modulators with 3.7-V-cm drive voltage at 1.55 $\mu$m were realized. The 1.94-$\mu$m-thick undoped GaAs–AlGaAs epilayer removed from its substrate behaves as an electrooptic dielectric layer and has electrodes placed directly on both sides. This allows a very strong modulating electric field overlapping very well with the optical mode. The propagation loss in the presence of electrodes is less than 2.9 dB/cm. There is very good agreement between the measured and simulated values.**

***Index Terms*—Electrooptic modulators, GaAs modulators, optical modulators.**

## I. Introduction

OPTICAL modulators are essential components for any fiber-optic system. As the penetration of fiber optics into communications systems and instrumentation increases, the demand for optical modulators will significantly increase. Modulator applications demand low cost, low drive voltage, low insertion loss, wide electrical and optical bandwidth, and adjustable chirp. At the present time, $LiNbO_3$ and electroabsorption modulators are commercially available. However, there is still a need for lower cost devices with lower drive voltages and wider electrical and optical bandwidths. Several electrooptic material systems including ferroelectric materials such as $BaTiO_3$ and $LiNbO_3$, compound semiconductors, and polymers are being actively researched to satisfy such requirements. Currently, ferroelectric materials and electrooptic polymers possess the largest electrooptic coefficient. However, the electrooptic coefficient is only one of several parameters that determine modulator performance. High index of refraction, advanced material growth, and device processing can easily enhance the performance while reducing the cost significantly. Compound semiconductors benefit in this regard even though they have smaller electrooptic coefficients. For example, substrate removal techniques make it possible to process both sides of an epilayer enabling the realization of an ideal push–pull modulator. In the past, we have demonstrated such bulk GaAs–AlGaAs modulators with a drive voltage of 8.7 V-cm [1]. In this letter, we report an optimized bulk GaAs–AlGaAs electrooptic modulator without any intentional doping. This modulator has a record low drive voltage of 3.7 V-cm at 1.55 $\mu$m.

Manuscript received June 15, 2006; revised August 1, 2006. This work was supported by National Science Foundation (NSF) Grant 442530-21379.

The authors are with the Electrical Engineering Department, University of California, Santa Barbara, CA 93106 USA (e-mail: jhshin@engineering.ucsb.edu; dagli@ece.ucsb.edu).

Digital Object Identifier 10.1109/LPT.2006.884729

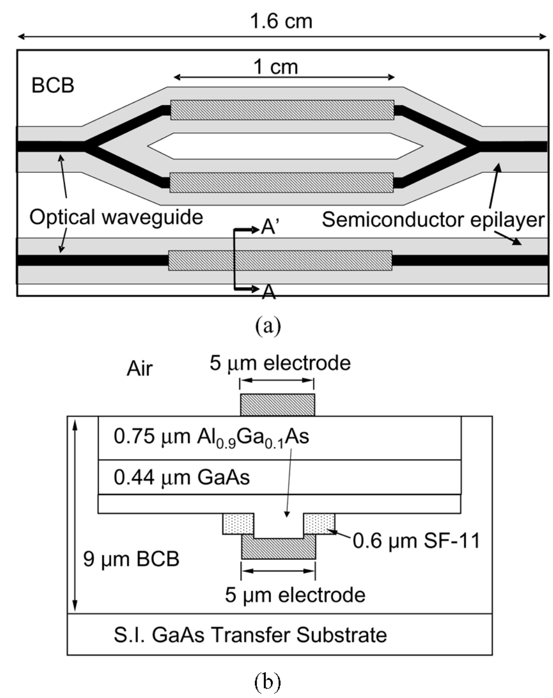


Fig. 1. (a) Top schematic of the device reported and (b) the cross-sectional schematic of the optical waveguide along A-A′. Note that the arms of the interferometer can be biased independently. For clarity, the contact pads for the top and bottom electrodes are not shown.

## II. Device Design and Description

Fig. 1 shows the top schematic of the device reported and the cross-sectional schematic of the optical waveguide used in this work. Both phase modulators and Mach–Zehnder intensity modulators are studied. Phase modulators also work as Fabry–Pérot modulators using facet reflections. The optical waveguide is a conventional rib waveguide. Vertical guiding is due to a three-layer slab waveguide. The epilayer containing the waveguide is separated from its substrate and glued onto a transfer substrate using benzocyclobutane (BCB) as glue. Furthermore, it is etched away where optical guiding is not needed. There are Schottky electrodes at the top and bottom of the optical waveguide. The epilayer is unintentionally doped and self depletes. Therefore, it is possible to treat it as a slightly lossy dielectric layer [1]. The electrodes on either side can be biased independently, hence, true push–pull operation is possible.

The drive voltage of a Mach–Zehnder modulator with push–pull drive can be expressed as

$$V_\pi = \frac{\lambda_0}{2L_e}\frac{t}{n_e^3 r_{41}}\frac{1}{\Gamma} \tag{1}$$

where $\lambda_0$ is the free space wavelength, $L_e$ is the length of the electrode, $n_e$ is the mode effective index, $r_{41}$ is the electrooptic coefficient, $t$ is the electrode gap, and $\Gamma$ is the overlap integral between the optical mode and the appropriate component of the applied electric field.

Based on (1), it is seen that minimizing $V_\pi$ requires minimizing $t$, maximizing $L_e, \Gamma, n_e$, and $r_{41}$. $n_e$ and $r_{41}$ depend on the material system used. In bulk compound semiconductors $r_{41}$ is low, but it can be increased significantly by using quantum wells with appropriate composition. Improvement by a factor of 3 without significant propagation loss has been recently reported utilizing this approach [2]. Even though $r_{41}$ is small, $n_e$ is around 3 and is much higher than other electrooptic material systems. Maximizing $L_e$ requires a low-loss optical waveguide. In this case, optical loss is mainly due to scattering from etched sidewalls and a small overlap with the metal electrodes. Loss due to material absorption and doping is negligible. In our design, the electrodes are placed on both sides of the epilayer as seen in Fig. 1(b), which makes the epilayer thickness $t$ the same as the electrode gap. This is a significant advantage since the epilayer thickness can be made very small and uniform. However, the optical mode should be contained entirely within the epilayer not to have any overlap with the metal electrodes on both sides of the epilayer. Any significant overlap with the metal electrodes would increase the optical propagation loss and limit the electrode length. Therefore, in the vertical direction, the mode size should be minimized. This can be achieved by increasing the index contrast between the core and cladding layers. This should be done while keeping the waveguide single-mode. In the AlGaAs material system, highest index contrast is obtained for a GaAs core and AlAs claddings. However, AlAs is not a very stable material, hence, claddings are chosen as $Al_{0.9}Ga_{0.1}As$. Once the core and cladding compositions are chosen, maximum core thickness that results in vertical single-mode operation is found. Then the cladding thickness is increased such that the optical field overlap with metal electrodes is less than 1%. This resulted in a 0.75-$\mu$m $Al_{0.9}Ga_{0.1}As$/0.44-$\mu$m GaAs/0.75-$\mu$m $Al_{0.9}Ga_{0.1}As$ epilayer. Maximizing $\Gamma$ requires a tightly confined optical mode in the lateral direction as well and a suitably chosen electrode width. In doing so, the waveguide should remain single-mode, low-loss, and easy to fabricate. For ease of fabrication and low propagation loss, the rib width was chosen as 2 $\mu$m. Then the etch depth was determined as 0.65 $\mu$m which is the maximum possible etch depth that still results in a single-mode waveguide. Furthermore, the overlap of the optical mode with the etched sidewall is minimized which helps to reduce the scattering loss. Next, the appropriate electrode width should be determined. For the given waveguide structure, calculations showed that increasing the electrode width beyond 5 $\mu$m had little effect on $\Gamma$ and $\Gamma$ saturates at 0.75. Therefore, the electrode width was chosen as 5 $\mu$m.

## III. Device Fabrication

Fabrication starts with the growth of a 0.75-$\mu$m $Al_{0.9}Ga_{0.1}As$/0.44-$\mu$m GaAs/0.75-$\mu$m $Al_{0.9}Ga_{0.1}As$ epilayer by molecular beam epitaxy on top of a thin AlAs layer on a GaAs substrate. There is a thin GaAs buffer layer between the bottom $Al_{0.9}Ga_{0.1}As$ layer and the AlAs etch stop layer. The GaAs buffer layer protects the AlAs layer during front side processing. First, the top $Al_{0.9}Ga_{0.1}As$ cladding layer is etched by reactive ion etching (RIE) with a $BCl_3$–$SiCl_4$ mixture to define single-mode optical waveguides. Next, a deep UV photoresist known as SF-11 is spun, planarized, and $O_2$ plasma-etched to expose the top surface of the ridge waveguide before metal contact formation. This step is required since the electrode is wider than the rib and needs some form of mechanical support. Next, 200 Å Ti/10 000 Å Au was evaporated directly on top of the ridge by photoresist liftoff to form the front Schottky electrodes. An RIE etch was performed to etch the semiconductor epilayer slightly into the GaAs buffer layer everywhere except where needed for optical guiding. This is followed by the deposition of so-called partial electrodes by liftoff. These electrodes provide access to the top electrodes after substrate removal. This step concludes the front side processing. Next, BCB is spun on the sample for planarization. The sample is then bonded upside down to another semi-insulating GaAs transfer substrate using BCB as a bonding layer. After curing the BCB, the epilayer growth substrate is removed by spray etching in a $NH_4OH:H_2O_2$ solution. During the spray etch AlAs layer serves as an etch stop layer to protect the device. After the spray etch AlAs layer is removed by HF. This is followed by etching the GaAs buffer layer using a citric-acid-based selective etch to expose the bottom $Al_{0.9}Ga_{0.1}As$ cladding layer. Finally, the backside 200Å Ti/10 000Å Au Schottky electrodes are formed on the $Al_{0.9}Ga_{0.1}As$ layer. The cross-sectional schematic of the completed waveguide is shown in Fig. 1(b).

## IV. Experimental Results

Both ends of the sample were cleaved and the output of a tunable laser at 1.55 $\mu$m was end fire coupled into the device through a cleaved fiber. During the measurements input polarization was maintained at TE. Optical alignment was achieved by observing the near-field pattern of the output light on an IR camera. Output power was measured by placing a photodetector in place of the camera. An iris was placed directly in front of the photodetector to minimize stray light coupling. The optical transfer function of the Mach–Zehnder modulator and its fit to the expected $\cos^2(\pi(V/2V_\pi))$ transfer function is shown in Fig. 2(a). This fit gave a $V_\pi$ value of 3.7$\pm$0.03 V-cm, which is in good agreement with the theoretical value of 3.7 V-cm based on (1). In this calculation, values used are $\lambda = 1.55$ $\mu$m, $t = 1.94$ $\mu$m, $\Gamma = 0.75$, $n_e = 3.23$, and $r_{41} = 1.6\text{pm}/V$.

$V_\pi$ can also be determined by making Fabry–Pérot measurements on phase modulators which are simply straight waveguides with electrodes [3]. The transmission of a Fabry–Pérot is given as

$$T = \frac{P_{\text{out}}}{P_{\text{in}}} = \frac{(1-r^2)^2 e^{-\alpha_T}}{(1-r^2 e^{-\alpha_T})^2 + 4r^2 e^{-\alpha_T} \sin^2\left(\frac{2\pi}{\lambda_0} n_e L + \frac{\pi}{2}\frac{V}{V_\pi}\right)}. \quad (2)$$

In this equation, $r^2$ is the facet reflectivity, $L$ is the chip length, and $\alpha_T$ is the on-chip propagation loss.

Results of Fabry–Pérot transmission measurements along with the fit to (2) are shown in Fig. 2(b). Based on fitting, $V_\pi$ was found to be 3.7$\pm$0.01 V-cm which is again in good agreement with the theoretical and Mach–Zehnder modulator values. The on-chip propagation loss was estimated using

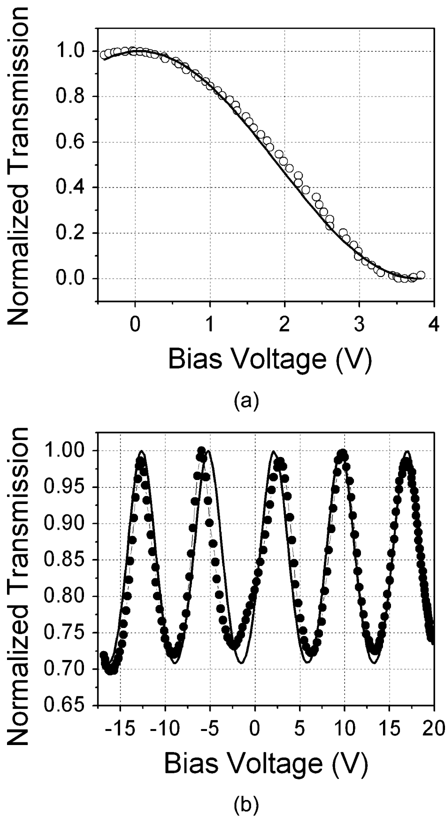


Fig. 2. (a) Measurement and $\cos^2(\pi(V/2V_\pi))$ fit of Mach–Zehnder modulator transmission as a function of applied voltage. (b) Measurement and fit of Fabry–Pérot transmission as a function of applied voltage. For both cases, the electrode length and the total device length were 1 and 1.6 cm, respectively.

fringe visibility $(T_{\max}/T_{\min})$ to be less than 2.9 dB/cm for devices with 1-cm-long electrodes. Furthermore, the optical loss measured on phase modulators with 0.5-cm-long electrodes was about 2.8 dB/cm. This indicates that the additional loss due to the electrodes is about 0.2 dB/cm which is well within the measurement error. Hence, additional loss due to the electrode is minimal. The loss quoted is the worst-case loss because the BCB layer between the transfer substrate and the epilayer also channels optical radiation. This radiation is not modulated when a voltage is applied to the optical waveguide and is hard to filter with the iris at the output. Therefore, $T_{\min}$ is enhanced and waveguide loss appears to be higher.

This device is not a high-speed modulator since it utilizes simple electrodes and its bandwidth would be limited by the resistance–capacitance (*RC*) time constant of the electrode. However, it is possible to make a high-speed modulator if the electrode were designed as a traveling-wave electrode similar to what is reported in [4].

## V. Conclusion

In this study, substrate removed GaAs–AlGaAs Mach–Zehnder and phase modulators were fabricated and characterized. By removing the growth substrate, independent electrodes were placed directly on top and bottom of the optical waveguide resulting in true push–pull operation. This dramatically increased the overlap between the optical mode and modulating electrical field and enabled 2-$\mu$m electrode gaps with excellent uniformity. The measured drive voltages were 3.7 V-cm, which is in excellent agreement with the calculated value. This is the lowest value reported for any GaAs electrooptic modulator at 1.55 $\mu$m. The on-chip propagation loss was measured to be less than 2.9 dB/cm. It was also found that electrodes had negligible effect on optical propagation loss. Increasing the electrooptic coefficient using InAlGaAs epilayers with quantum wells [2] and utilizing electrode designs similar to those in [4] would enable very high-speed intensity modulators with drive voltage less than 1 V.

## References

[1] S. R. Sakamoto, A. Jackson, and N. Dagli, "Substrate removed GaAs/AlGaAs electro-optic modulators," *IEEE Photon. Technol. Lett.*, vol. 11, no. 10, pp. 1244–1246, Oct. 1999.

[2] K. Tsuzuki, T. Ishibashi, T. Ito, S. Oku, Y. Shibata, R. Iga, Y. Kondo, and Y. Tohmori, "40 Gbit/s n-i-n InP Mach–Zehnder modulator with a $\pi$ voltage of 2.2 V," *Electron. Lett.*, vol. 39, no. 20, pp. 1464–1466, Aug. 7, 2003.

[3] J. H. Shin, S. Wu, and N. Dagli, "Substrate removed low drive voltage GaAs/AlGaAs semiconductor electro-optic phase modulators," in *Proc. Integrated Photonics Research Conf.*, San Francisco, CA, Jun. 30–Jul. 2 2004, Paper IThD-3.

[4] J. H. Shin, C. Ozturk, S. R. Sakamoto, Y. J. Chiu, and N. Dagli, "Novel T-rail electrodes for substrate removed low-voltage, high-speed GaAs/AlGaAs electro-optic modulators," *IEEE Trans. Microw. Theory Tech.*, vol. 53, no. 2, pp. 636–643, Feb. 2005.